

SPIE PRESS



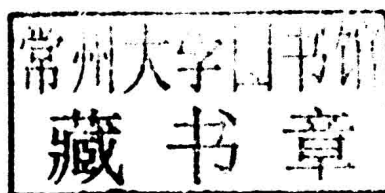
SPIE

Chemical Vapor Deposited **Zinc Sulfide**

John McCloy and Randal Tustison

Chemical Vapor Deposited **Zinc Sulfide**

John McCloy and Randal Tustison



SPIE
PRESS

Bellingham, Washington USA

Library of Congress Control Number Data

McCloy, John

Chemical vapor deposited zinc sulfide / John McCloy and Randal Tustison.
p.; cm.

Includes bibliographical references and index.

ISBN 978-0-8194-9589-1

1. Chemical vapor deposition. 2. Zinc sulfide. 3. Chemical processes--infrared materials. I. Title.

TP1750.W55 2013

542-dc23

2013932605

Published by

SPIE—The International Society for Optical Engineering

P.O. Box 10

Bellingham, Washington 98227-0010 USA

Phone: +1 360 676 3290

Fax: +1 360 647 1445

Email: spie@spie.org

Web: <http://spie.org>

Copyright © 2013 Society of Photo-Optical Instrumentation Engineers (SPIE)

All rights reserved. No part of this publication may be reproduced or distributed in any form or by any means without written permission of the publisher.

The content of this book reflects the work and thought of the author(s). Every effort has been made to publish reliable and accurate information herein, but the publisher is not responsible for the validity of the information or for any outcomes resulting from reliance thereon.

Printed in the United States of America.

First printing



Chemical Vapor Deposited
Zinc Sulfide

Preface

Zinc sulfide (ZnS) has shown unequaled utility for infrared windows that require a combination of long-wavelength infrared (8–12 μm) transparency, mechanical durability, and elevated temperature performance. Its unique set of properties extends its usefulness to electroluminescent phosphors, optical thin films used for filters and antireflection (AR) coatings, as well as various other opto-electronic applications. High-optical-quality, chemical vapor deposited ZnS windows several millimeters thick transmit visible light and so have received attention as candidates for multi-spectral windows.

Naturally occurring zinc sulfide is well known as the primary ore of zinc. The common names for the cubic form of ZnS all come from its superficial resemblance to galena (lead sulfide, PbS), but ZnS does not yield any metal when smelted. It was therefore called “blende” or “zincblende” (from the German *blenden*, “to deceive” or “to blind”), or “sphalerite” [from the Greek σφαλερός (*sphaleros*), “deceptive” or “treacherous.”]¹ A special white, transparent, or colorless variety of sphalerite from Franklin, New Jersey, and Nordmark, Sweden, is called cleiophane, which is nearly pure ZnS with only traces of cadmium. Mineral sphalerite tends to have a large component of iron and manganese, and some specimens are very black, so-called “black jack.” Mineral cleiophane and sphalerite exhibit different-colored fluorescence under short-wavelength and long-wavelength ultraviolet light, and are of interest to the mineral collector. Wurtzite is a less common hexagonal form of ZnS, named after the French chemist Charles-Adolphe Wurtz (1817–1884) by C. Friedel when it was first identified from a Bolivian silver mine. Mineral hexagonal zinc sulfide containing significant amounts of cadmium is known as pribramite. Hexagonal zinc oxysulfide has been called voltzite or voltzine, though these terms have been used to describe a lead oxysulfide as well.

Bulk ZnS for infrared windows is traditionally manufactured by chemical vapor deposition (CVD) in large reactors. Deposition temperature and mole fractions of the reactants, H₂S gas and Zn vapor, have a large influence on

¹ Mellor, J.W., “Zinc and Cadmium Sulphides,” in *A Comprehensive Treatise on Inorganic and Theoretical Chemistry*, 586–612, Longmans, Green, and Co., London (1956).

visible scatter and absorption. These effects have been ascribed to electronic defects in the bandgap, hexagonal phase ZnS, and residual porosity, but the exact mechanisms have never been adequately explained.

A multispectral form of ZnS can be created by taking traditionally grown polycrystalline CVD ZnS, which is visibly yellow and opaque, and subjecting it to a post-deposition heat treatment under pressure. The heat and pressure result in recrystallization of the CVD ZnS, large grain growth, and a visibly clear and colorless product. The kinetics of this post-process, as well as the dependence on the platinum foil that typically encases the ZnS during heat treatment, remain poorly understood. It is known that CVD materials grown under different conditions do not behave identically when subsequently heat treated.

The purpose of this book is to review the physical properties of CVD ZnS and their relationship to the chemical vapor deposition process that produced them. We begin with the physics and chemistry of ZnS itself, including its many polytypes. This establishes a basis for understanding the defect structure and how it influences observed properties. Attention is then turned to the CVD process and the resulting forms of ZnS with properties that vary widely with processing conditions. To understand these variations, an in-depth look at the material microstructure follows, including the effects of post-deposition heat treatments.

For optical applications, the optical transmittance is of primary importance. ZnS intrinsically exhibits very broadband transparency beginning in the ultraviolet and extending through the infrared. This intrinsic transparency, coupled with modest mechanical durability, makes it unique among available infrared window materials. CVD ZnS optical properties are discussed, including the effects on these optical properties of post-deposition heat treatment, with comments on mechanisms for transparency improvements.

Finally, because the CVD process itself is central to the development of this material, a brief history of this process is presented, beginning with its use in the 19th century as a coating technology. The evolution of CVD as a bulk-materials process came later, and only by the mid-twentieth century was it beginning to be utilized to produce CVD-formed products (most notably pyrolytic graphite). This development was an important milestone, as it put in place the process technology that was critical to the subsequent development of CVD ZnS. We offer this information as a historical note to explain the success of the CVD ZnS process as well as subsequent improvements in the process, including post-deposition heat treatments, but will not focus explicitly on the CVD process technology used to produce ZnS commercially today.

*John McCloy
Randal Tustison
March 2013*

Acknowledgments

We would like to thank the University of Arizona, particularly Prof. Donald Uhlmann, for providing the opportunity to gather much of the material contained in this book in preparation of a doctoral thesis (McCloy, 2008), and Raytheon Company for allowing and encouraging its publication. Of course, this book would not be possible without the many contributions from our current and former colleagues and their work on this subject. In particular we have benefited from discussions with Barney DiBenedetto and Chuck Willingham, both of whom were instrumental in the development of CVD ZnS, as well as the late Jim Pappis who was a mentor and friend to many of us. This text also benefitted from conversations with Stan Waugh, Tony Capriulo, and Andre Morrisette, as well as access to Raytheon Company archival material in reconstructing the development of CVD ZnS at Raytheon. Many colleagues at Raytheon and elsewhere have assisted us over the years in collecting the data presented herein, and they are too numerous to list here.

The authors would also like to acknowledge the reviewers of the manuscript, whose thorough reading and insightful comments added to this text. We also thank the editors from SPIE Press, especially Scott McNeill, who turned our manuscript into this book. Any remaining errors are ours, and we encourage the finding of these to be brought to our attention at jsmccloy@alum.mit.edu for correction.

Finally and most importantly, we thank our families for their support during the preparation of this book, especially our wives, Kay Tustison and Christy McCloy, for their patience and encouragement. Much of what we do would not be possible otherwise.

Contents

<i>Preface</i>	ix
<i>List of Figures</i>	xi
<i>List of Tables</i>	xiii
<i>Acknowledgments</i>	xvii
1 Physics and Chemistry of ZnS	1
1.1 Crystallography	1
1.1.1 Stoichiometry and oxygen impurity	2
1.1.2 Detailed crystallography and lattice parameter	3
1.1.3 Polytypes and hexagonality	5
1.1.4 Phase transformation and twinning	9
1.2 Electronic and Vibrational Structure	11
1.2.1 Electronic structure	11
1.2.2 Vibrational structure	14
1.3 Important Defects and Chemistry	16
1.3.1 Native defects	16
1.3.2 Oxygen impurity	18
1.3.3 Hydrogen impurity	19
1.3.4 Transition metals	20
References	21
2 Technical Issues in Processing of CVD ZnS	31
2.1 Introduction	31
2.1.1 Vapor phase equilibrium	32
2.2 Chemical Vapor Deposition of ZnS	34
2.2.1 Homogeneous and heterogeneous CVD reactions	35
2.2.2 Commercial CVD reactor considerations	36
2.2.2.1 Mandrels	37
2.2.2.2 Deposition stress and thickness uniformity	38
2.2.2.3 Deposition temperature, pressure, and reactant ratios	38
2.2.2.4 Deposition rate	39
2.2.2.5 Porosity	40
2.2.3 Summary	41
2.3 Heat Treatment of CVD ZnS	41

2.3.1	Annealing	42
2.3.2	Hot pressing and sintering of ZnS powders	43
2.3.3	Hot isostatic pressing	44
2.3.3.1	Creep, densification, and diffusion	45
2.3.3.2	Considerations for commercial HIPing of CVD ZnS	46
2.3.4	Summary	47
	References	47
3	Structure and Microstructure	53
3.1	Atomic Structure	53
3.1.1	X-ray diffraction	54
3.1.1.1	Polycrystalline sample diffraction and texture	54
3.1.1.2	Powder diffraction and hexagonality	59
3.1.2	Electron diffraction	60
3.2	Nanostructure and Microstructure	64
3.2.1	Recrystallization as a result of heat treatment of CVD ZnS	67
3.2.2	Effects of HIP on mechanical properties	71
3.3	Mesostructure and Macrostructure	72
	References	76
4	Optical Transmission	81
4.1	Experimental Transmission Curves	83
4.1.1	Single-crystal ZnS	83
4.1.2	Polycrystalline ZnS, no postprocessing	85
4.1.3	Heat treated and HIPed samples	90
4.2	Mechanisms for Transmission Improvement	91
4.2.1	Isothermal heat treatment	92
4.2.2	Hot isostatic pressing	92
	References	93
5	The Development of Chemical Vapor Deposited ZnS	97
5.1	Chemical Vapor Deposition	97
5.2	Raytheon High-Temperature Materials	99
5.3	Raytheon CVD ZnS	103
5.4	Multispectral ZnS and Elemental ZnS	110
5.5	"Improvements" to CVD ZnS: Composites with ZnGa ₂ S ₄ and Diamond	115
5.6	Applications of CVD ZnS	116
	References	117
6	Perspective and Future Work	123
6.1	What Is The Nature of Standard CVD ZnS?	123
6.1.1	What is red ZnS?	125
6.1.2	What is elemental ZnS?	127

6.2	What Is the Nature of Transformation to Multispectral ZnS?	128
6.2.1	What is the HIP doing?	129
6.2.2	What is the metal doing?	131
6.3	Conclusions	133
6.4	Suggestions for Future Work	134
6.5	Final Thoughts	136
	References	137
Appendix	Engineering Data	141
A.1	Table of ZnS Engineering Properties	141
A.2	Elastic Properties	141
A.2.1	Density	141
A.2.2	Young's modulus and Poisson's ratio	142
A.3	Mechanical properties	143
A.3.1	Hardness	145
A.3.2	Toughness	146
A.3.2.1	Slow crack growth	148
A.3.3	Fracture strength	150
A.3.4	Rain and sand erosion resistance	151
A.3.5	Laser-damage effects	152
A.4	Thermal Properties	152
A.4.1	Thermal expansion	152
A.4.2	Thermal conductivity	153
A.4.3	Specific heat (heat capacity)	153
A.5	Optical Properties	153
A.5.1	Refractive index	153
A.5.2	Thermo-optic coefficient	155
A.5.3	Absorption coefficient	156
A.5.4	Dielectric constant	162
A.5.5	Scattering	164
	References	165
<i>Index</i>		171

List of Figures

Figure 1.1	Wurtzite (left) and sphalerite (right) structures	4
Figure 1.2	Unit cells of (left) 3C ZnS (sphalerite) and (right) 2H ZnS (wurtzite)	7
Figure 1.3	Polytype 10 H with 20% hexagonality	8
Figure 1.4	Band structure of sphalerite and wurtzite ZnS at zone center	11
Figure 1.5	Energy band structure and density of states for sphalerite and wurtzite ZnS	12
Figure 1.6	Cubic ZnS by LCAO method	12
Figure 1.7	Hexagonal ZnS by <i>ab initio</i> local density approximation	13
Figure 1.8	Phonon density of states for ZnS and calculated dispersion	14
Figure 1.9	10-parameter valence-shell phonon model based on neutron diffraction data for ZnS	14
Figure 2.1	Calculated partial pressure of species in a ZnS chemical vapor reaction in the presence of hydrogen (left) or water (right)	33
Figure 2.2	Evidence of gas phase nucleation of $\text{ZnS}_x\text{Se}_{1-x}$ particles which then stick to hexagonal needles and become incorporated into bulk CVD material	35
Figure 2.3	Illustration of the proposed model of ZnS growth; H_2S adsorbs to the surface and reacts with Zn	36
Figure 2.4	Schematic of ZnS reactor	37
Figure 2.5	Grain size versus CVD deposition temperature and HIP temperature	38
Figure 2.6	Grain size evolution with deposition temperature	39
Figure 3.1	Hierarchies of structure in CVD ZnS	53
Figure 3.2	X-ray diffraction of polycrystalline specimens of ZnS	54
Figure 3.3	XRD comparisons for CVD versus HIP CVD	58
Figure 3.4	Close-up of powder XRD showing the regions used for consideration of hexagonality	59
Figure 3.5	Comparison of XRD texture, hexagonality (α), and optical extinction measured at $1.064\ \mu\text{m}$ (β_{ext}) for various samples	61
Figure 3.6	Variation in XRD spectra with respect to position in the growth direction	61
Figure 3.7	Raytheon ZnS 60-k \times TEM and SAED of highly twinned region	62

Figure 3.8	Princeton Scientific ZnS 40-k \times TEM and SAED of two regions	63
Figure 3.9	CVD ZnS (left) versus HIPed CVD ZnS (right) at various length scales	65
Figure 3.10	TEM image of Raytheon CVD ZnS	66
Figure 3.11	Etched, heat-treated ZnS samples recrystallized without metal	68
Figure 3.12	Recrystallization of sample exposed to Cu foil in 900 °C interrupted HIP	69
Figure 3.13	Macroscopic features in polished CVD ZnS	73
Figure 3.14	Nodular growth on the surface of CVD ZnS away from the mandrel	74
Figure 3.15	Interferometric images of opposite sides of a 20-mm thick CVD ZnS disk after removing 1.5 μ m using magnetorheological finishing	74
Figure 3.16	110-MHz scanning acoustic microscope images	75
Figure 4.1	Transmission of ZnO, ZnS, and ZnSe	84
Figure 4.2	Band-edge transmission of ZnO, ZnS, and ZnSe	84
Figure 4.3	CVD ZnS transmission	87
Figure 4.4	ZnS transmission	87
Figure 4.5	Transmission of ZnS in the vicinity of the hydride absorption	88
Figure 4.6	Extrinsic infrared absorptions in ZnS samples	89
Figure 4.7	Transmission curves compared for 750 °C, 16 h with various metals	90
Figure 4.8	Calculated band-edge extinction for CVD ZnS and heat-treated samples	99
Figure 5.1	The Aylsworth vapor deposition system for coating carbon lamp filaments	100
Figure 5.2	One of the 4-inch-diameter experimental reactors used to develop the pyrolytic graphite deposition process	101
Figure 5.3	Various PG components, including rocket nozzles and nozzle inserts produced by the HTM Department	101
Figure 5.4	A 6" internal diameter, PG deposition reactor in Raytheon's HTM pilot plant, circa 1960	102
Figure 5.5	A large-scale, PG deposition reactor in Raytheon's HTM plant	102
Figure 5.6	A schematic representation of a dynamic CVD deposition system	104
Figure 5.7	The exploratory ZnS CVD system	105
Figure 5.8	Infrared transmittance of CVD ZnS from exploratory deposition ZS-23	106
Figure 5.9	The resistance furnaces used to develop the CVD ZnS process	108
Figure 5.10	Installation of the first 52" production furnace	109
Figure 5.11	34" \times 34" \times 9" mandrel box with five by-flow H ₂ S nozzles	110
Figure 5.12	Loading the deposition mandrel and fixturing into the ZnS reactor	111
Figure 5.13	Inspection of large 34" \times 34" CVD ZnS plate	111
Figure 5.14	Raytheon's CVD production facility in Waltham, MA	112
Figure 5.15	A large CVD ZnSe laser window produced at Raytheon, demonstrating the size and optical quality capability of the CVD process	112

Figure 5.16	The current elemental ZnS (or eZnS [®]) processing facility at Raytheon Company	114
Figure 6.1	Standard CVD ZnS (left) and multispectral ZnS (right) produced commercially at Raytheon	137
Figure A.1	Hardness as a function of grain size	145
Figure A.2	Fracture toughness as a function of grain size	147
Figure A.3	ZnS biaxial flexure probability of failure versus applied stress	150
Figure A.4	Refractive index versus wavelength (nm) based on Sellmeier equations from Li and Klein	155
Figure A.5	Refractive index versus wavenumber (log scale) and versus wavelength (μm)	156
Figure A.6	dn/dT of multispectral ZnS	157
Figure A.7	Extinction coefficient (imaginary refractive index, log scale) versus wavenumber (log scale) and wavelength	159
Figure A.8	Experimental absorption coefficient of multispectral ZnS as a function of temperature	160
Figure A.9	Transmittance of CVD ZnS and assignment of multiphonon modes	161
Figure A.10	Absorption coefficient as a function of wavenumber for ZnS with major phonon assignments	162

